smll.201600243

Chemical signaling and functional activation in colloidosome-based protocells

Shiyong Sun, Mei Li, Faqin Dong, Shengjie Wang, Liangfei Tian, and Stephen Mann**

Dr S. Sun, Dr. M. Li, Dr S. Wang, Dr L. Tian, Prof. S. Mann
Centre for Protolife Research and Centre for Organized Matter Chemistry,
School of Chemistry,
University of Bristol,
Bristol BS8 1TS, UK.
Email: s.mann@bristol.ac.uk; mei.li@bristol.ac.uk

Dr S. Sun , Dr F. Dong
School of Environment and Resource,
Key Laboratory of Solid Waste Treatment and Resource Recycle,
Southwest University of Science and Technology,
Mianyang, Sichuan 621010, China.

Dr S. Wang
Centre for Bioengineering and Biotechnology, China University of Petroleum, Qingdao 266580, China.

An aqueous-based micro-compartmentalized model involving the integration of partially hydrophobic Fe(III)-rich montmorillonite (FeM) clay particles as structural and catalytic building blocks for colloidosome membrane assembly, self-directed membrane remodeling and signal-induced protocell communication is described. The clay colloidosomes exhibit size- and charge-selective permeability, and show dual catalytic functions involving spatially confined enzyme-mediated dephosphorylation and peroxidase-like membrane activity. The latter is used for the colloidosome-mediated synthesis and assembly of a temperature-responsive poly(N-isopropylacrylamide)(PNIPAM)/clay integrated hybrid membrane. In situ *PNIPAM elaboration of the membrane is coupled to a glucose oxidase (GOx)-mediated signaling pathway to establish a primitive model of chemical communication and functional activation within a synthetic "protocell community" comprising a mixed population of GOx-containing silica colloidosomes and alkaline phosphatase (ALP)-containing FeM-clay colloidosomes. Triggering the enzyme reaction in the silica colloidosomes gives a hydrogen peroxide signal that induces polymer wall formation in a coexistent population of the FeM-clay colloidosomes, which in turn generates self-regulated membrane-gated ALP-activity within the clay micro-compartments. The emergence of new functionalities in inorganic colloidosomes via chemical communication between different protocell populations provides a first step towards the realization of interacting communities of synthetic functional micro-compartments.*

1. Introduction

The design and assembly of membrane-bounded semi-permeable micro-compartments is becoming increasingly relevant to diverse areas of materials research such as the development of new types of functional microscale ensembles,[1,2] and chemical construction of rudimentary models of synthetic cellularity (protocells).[3,4] In this regard, the spontaneous partitioning of colloidal particles at water/oil interfaces to produce Pickering emulsion droplets comprising shell-like micro-structures provides a straightforward procedure for the self-assembly of robust, semi-permeable microcapsules (colloidosomes) with potential uses in a wide range of micro-encapsulation and micro-reactor technologies.[5-9] Recent studies have indicated that water-in-oil inorganic colloidosomes can be prepared from hydrophobically modified particles of amorphous silica,[10] mesoporous silica,[11] or laponite.[12,13] Significantly, the as-prepared silica-stabilized emulsion droplets can be exploited as membrane-bounded micro-compartments for enhanced enzyme-mediated transformations,[14,15] or cross-linked and transferred into a continuous water phase for use as colloidosome-based protocell models for integrating various biomimetic or biological processes, including cytoskeletal-like hydrogel assembly,[16] capsule growth and division,[17] synthesis of RNA and proteins via cell-free gene expression pathways,[15] and membrane gating of encapsulated enzyme reactions.[18] Water-in-water clay colloidosomes have also been prepared using unmodified montmorillonite particles by applying wetting procedures to clay-coated air bubbles suspended in water.[19]

Although many reports have addressed the stability and release properties of colloidosomes,[20-23] there are relatively few investigations concerning the construction of these micro-capsules from functional nanoscale building blocks. Notably, cubic particles of a metal-organic coordination compound[24] and nanoparticles of mesoporous silica[11] have been used to prepare colloidosomes exhibiting type I or IV microporosity, respectively, and catalytically active Pickering emulsions have been constructed from silica building blocks decorated with gold[11] or palladium[25,26] nanoclusters.

In this paper, we describe the preparation and use of novel cross-linked water-in-water clay-based colloidosomes that exhibit dual catalytic functionality based on their membrane structure and composition, and ability to encapsulate functional enzymes. The catalytic membrane is generated from the emulsion-based assembly of partially hydrophobic particles of a Fe(III)-enriched montmorillonite (nontronite; FeM-clay), which has a 2:1 smectite group structure with Fe(III) ions mainly located in the octahedral sites, and a total iron content of approximately 25 wt%.[27,28] We demonstrate three properties of this new system. Firstly, we exploit the catalytically active colloidosomes for the self-directed peroxidative polymerization of N-isopropylacrylamide (NIPAM), which occurs specifically at the surface of the FeM-clay membrane to produce inorganic protocells enveloped in a temperature-responsive poly(N-isopropylacrylamide) (PNIPAM) wall.

Secondly, we couple the potential for *in situ* PNIPAM elaboration of the semi-permeable FeM-clay membrane with a glucose oxidase (GOx)-mediated signaling pathway to develop a primitive model of chemical communication within a synthetic "protocell community" comprising a mixed population of silica and FeM-clay colloidosomes. Specifically, we initiate the enzyme reaction within a population of GOx-containing silica colloidosomes to generate a hydrogen peroxide signal that diffuses through the medium and induces PNIPAM wall formation in a coexistent population of FeM-clay colloidosomes. As a consequence, the membrane structure and properties of the FeM-clay colloidosomes are remodeled by the activity of the silica microcapsules. Thirdly, we exploit the chemical communication process to introduce new protocell functions in the reconfigured FeM-clay colloidosomes. In particular, by encapsulating alkaline phosphatase (ALP) within the PNIPAM-functionalized FeM-clay microcapsules we show that the remodeled clay colloidosomes adopt temperature-dependent membrane-gating properties with respect to a small molecule substrate (*p*-nitrophenyl phosphate), indicating that the signaling pathway can be coupled to the activation of new biomimetic functions.

In general, the demonstration that new properties emerge in subsets of colloidosome populations by internal signaling could provide a first step towards establishing interacting synthetic communities of functional microcapsules. Such artificial communities could have potential use as multiplex micro-reactor networks in biomimetic engineering and synergistic sensing systems, and in the realization of collective behavior in protocell consortia.

2. Results and discussion

2.1 Preparation and properties of Fe-rich montmorillonite colloidosomes

A sample of partially hydrophobic FeM-clay was prepared by covalent coupling of methyltriethoxysilane to accessible hydroxyl groups of a swollen surfactant-intercalated FeM-clay precursor (see Methods) to produce sheet-like *ca.* 1 μm-sized micro-particles (Figure S1a,b) that aggregated at the interface between water and cyclohexane (Figure S1c). The contact angle for water droplets mounted on samples of the surface-alkylated FeM-clay was *ca.* 63^{o} (Figure S1d,e), consistent with hydrophobic modification of the inorganic structure. FTIR spectra confirmed the presence of methyl groups (CH stretching at 2800-2900 cm^{-1}) in the organically modified clay (Figure S2, Table S1), and XRD profiles indicated that the interlayer space was cross-linked by silylation such that the methyl-functionalized FeM-clay particles did not undergo exfoliation in the presence of bovine serum albumin (BSA) (Figure S3, Table S2). Zeta potential measurements of FeM-clay suspensions in 10% ethanol/water mixtures before and after methylation gave negative surface potentials, with values of approximately -18 and -12 mV, respectively (Table S3).

Partially hydrophobic methylated FeM-clay micro-particles were used to prepare

water-in-oil Pickering emulsions in cyclohexane or dodecane at a typical water/oil volume fraction of 0.05 and water/FeM-clay volume/weight ratio of 100 µL mg^{-1}. The resulting emulsion droplets were structurally robust, spherical in morphology, and polydisperse in size with a mean diameter of 110 µm (Figure 1a; Figure S4). No coalescence of the droplets was observed in emulsions stored for several months. Self-assembly and preferential localization of the organically modified FeM-clay at the water/oil interface were confirmed by polarized light microscopy, which showed the presence of birefringence associated specifically with the droplet surface (Figure 1b). Transfer of the FeM-clay stabilized emulsion droplets into water was undertaken by cross-linking the inorganic membrane by reaction with tetramethoxysilane (TMOS), followed by treatment with a series of ethanol/water solvents. These procedures gave aqueous suspensions containing a high yield of intact FeM-clay colloidosomes that retained their membrane-associated birefringence (Figure 1c,d). SEM examination of the dried or freeze-fractured colloidosomes showed, respectively, individual micro-capsules that were structurally robust under vacuum (Figure 1e), or a hollow interior and continuous clay membrane that was several micrometers in thickness, roughened in texture and highly creased (Figure 1f,g). The average size of the FeM-clay colloidosomes was dependent on the water/clay volume/weight ratio used in the preparations; for example, changing the ratio from 50 to 250 µL mg^{-1} increased the average size of the micro-compartments from 30 to 350 µm (Figure 1h).

In light of previous studies on the use of silica colloidosomes as a potential model of an inorganic protocell[15-18], we investigated the encapsulation properties and membrane permeability of the FeM-clay micro-capsules. A range of small-molecule dyes, fluorescent proteins and DNA polynucleotides could be readily encapsulated within the FeM-clay water-in-oil Pickering emulsions without disruption of the interfacial assembly process or leakage into the oil phase (Figure 2a-f). In addition, studies of the uptake of solute molecules into water-in-water colloidosomes indicated that the negatively charged FeM-clay membrane was both surface-active and semi-permeable. Positively charged dye molecules such as Rhodamine B were electrostatically bound to the FeM-clay shell to produce colloidosome membranes with high fluorescence intensity (Figure 2g), whereas negatively charge dyes such as fluorescein isothiocyanate (FITC) and calcein were passively taken up into the interior of the inorganic micro-compartments (Figure 2h,i). Significantly, the porous FeM-clay membrane was impermeable to globular proteins (GFP; *ca*. 2 nm in size) and anionic polynucleotides (dsDNA, ~2000 base pairs) (Figure 2j-l).

2.2 Membrane-mediated catalysis and polymer wall assembly

The combination of selective small-molecule permeability and retention of biological macromolecules suggested that the FeM-clay colloidosomes could be used as inorganic

protocell models to house biomimetic processes. In this regard, we investigated whether the intrinsic catalytic properties of the FeM-clay micro-particles could be exploited for the self-directed synthesis and self-assembly of a polymer corona on the inorganic membrane. For this, we first demonstrated that the partially hydrophobic FeM-clay particles, as well as the cross-linked colloidosomes in water, were catalytically active in the oxidation of 3,3',5,5'-tetramethylbenzidine (colourless) to 3,3',5,5'-tetramethylbenzidine diimine (blue) via decomposition of H_2O_2 and formation of hydroxyl free radicals (Figures S5,6,7). We then exploited the intrinsic reactivity of the colloidosomes for inducing the peroxidative polymerization of NIPAM specifically at the interface with the FeM-clay membrane with the aim of producing inorganic protocells with a temperature-responsive polymer wall. Hydrogen peroxide (H_2O_2), NIPAM, fluorescein *o*-acrylate (FOA; 1%; green fluorescence co-monomer) and PEG-diacrylate (PEG-DA; crosslinker) were added to the external aqueous phase of a suspension of water-in-water FeM-clay colloidosomes, and the dispersions typically left at room temperature for 24 h. Scanning electron microscopy (SEM) images of ethanol-washed and dried samples showed the presence of a film-like adherent layer on the surface of the intact FeM-clay colloidosomes (Figure 3a). Corresponding EDX analyses gave peaks for Fe, and showed an increased carbon content compared to the partially hydrophobic FeM-clay micro-particles alone (Figure S8), suggesting that the colloidosomes were enveloped in a shell of PNIPAM. Confocal laser scanning microscopy was used to confirm the presence and spatial location of the FOA-doped PNIPAM polymer. Colloidosomes isolated after reaction times of 24 h exhibited high intensity FOA-derived green fluorescence specifically in association with the FeM-clay shell (Figure 3b). In contrast, control experiments showed no qualitative evidence for H_2O_2-mediated NIPAM polymerization in the absence of FeM-clay particles or FeM-clay colloidosomes (Figure S9), and no polymerization was observed when FeM-clay colloidosomes were incubated with a mixture of FOA and NIPAM in the absence of H_2O_2 (Figure S10).

Taken together, the above observations were consistent with preferential polymerization of the organic monomer at the surface of the inorganic membrane to produce colloidosomes with a hybrid shell structure consisting of closely packed silica-cross-linked FeM-clay platelets and a thin adherent film of PEG-DA cross-linked PNIPAM. Heating the PNIPAM/FeM-clay colloidosomes in water above the reversible lower critical solution temperature (LCST) of PNIPAM (32°C) increased the fluorescence intensity associated with the membrane without changing the size of the colloidosomes (Figure 3c). We attributed this to entropically induced deswelling of the polymer matrix attached to the FeM-clay membrane, such that the PNIPAM shell transformed from an expanded (hydrophilic) state into a contracted (hydrophobic) conformation as the temperature was increased above the LCST. These observations suggested that the hybrid colloidosomes should be capable of temperature-dependent stimulus-responsive behavior under

appropriate environmental conditions.

2.3 Chemical communication and functional activation in mixed colloidosome populations

Having established that polymer-enveloped FeM-clay colloidosomes could be prepared by self-directed catalytic activity in the presence of H_2O_2, we used this process as the basis of a design strategy to couple the functionality of different colloidosome populations via a simple signaling pathway. Our objective was to develop a primitive model of chemical communication and functional activation in which the triggering of an enzyme reaction in population **I** results in the signal-mediated induction of polymer wall formation in population **II** and the subsequent emergence of new membrane-mediated properties in this subset of remodeled colloidosomes (population **II***) (Figure 3d). Specifically, population **I** consisted of GOx-containing colloidosomes prepared with a cross-linked, chemically passive silica nanoparticle membrane, whilst those in population **II** comprised the catalytically active FeM-clay colloidosomes, which in some experiments contained encapsulated alkaline phosphatase (ALP) (see below). The silica colloidosomes were permeable to small molecules but not to proteins and enzymes, and have been extensively characterized in previous studies.[10,15,18] We also encapsulated Rhodamine B-labeled bovine serum albumin along with GOx within the silica colloidosomes to visually distinguish between the different types of protocells in reaction solutions containing NIPAM, FOA (1%) and PEG-DA. Confocal laser scanning microscopy images of the combined populations showed a mixture of relatively small red fluorescent silica colloidosomes with diameters generally less than 75 μm, along with much larger non-fluorescent FeM-clay colloidosomes that were 150 μm or so in size (Figure S11a). Glucose was then added to the reaction suspension to initiate GOx-mediated formation of H_2O_2 within the silica colloidosomes followed by subsequent release of H_2O_2 molecules into the aqueous continuous phase. Correspondingly, samples imaged 9 h after addition of glucose showed a progressive increase in green fluorescence associated specifically with the membrane of the FeM-clay colloidosomes, along with a concomitant reduction in the background green fluorescence originating from the FOA monomer in the continuous phase (Figure S11b). Green fluorescence was not observed in association with the silica colloidosomes. As a consequence, diffusion of H_2O_2 from the silica colloidosomes and subsequent triggering of the synthesis and assembly of a PNIPAM/FOA polymer layer on the membrane of the FeM-clay colloidosomes produced a binary population of discrete red and green microcapsules within a period of 24 h. (Figure 3e). In contrast, PNIPAM synthesis was not induced in the absence of glucose (Figure S12), confirming that the chemical activity of population **I** along with diffusion of the H_2O_2 reaction product were prerequisites for membrane remodeling in **II.**

Given that signaling from the silica colloidosomes gave rise to *in situ* structural modifications in the FeM-clay micro-compartments, we investigated whether this process of selective adaptation could be exploited to introduce new protocell functions in the reconfigured microcapsules. In this regard, we investigated how the above communication pathway influenced the activity of ALP molecules entrapped within the FeM-clay colloidosomes. The small molecule substrate, *p*-nitrophenyl phosphate (pNPP) was added to a mixed population of the red and green fluorescent colloidosomes 24 h after initiation of the cascade reaction, and the initial rate of enzyme-mediated dephosphorylation associated with the production of the yellow product 4-nitrophenolate (4NP) from within the ALP-containing PNIPAM/FeM-clay colloidosomes measured spectroscopically. The enzyme assays were performed at temperatures between 25 and 40°C. Significantly, plots of the initial rates of enzyme-catalyzed dephosphorylation against temperature showed a progressive increase up to 34^{o}C, above which the reaction rate decreased (Figure 3f). In contrast, control experiments carried out under the same conditions but in the absence of NIPAM, such that the FeM-clay colloidosomes remained polymer-free, showed a continued increase in the initial reaction up to 40^{o}C (Figure 3f). The results implied that the decrease in the initial rate of the dephosphorylation reaction within the PNIPAM/FeM-clay protocells above 34^{o}C was not associated with temperature-induced denaturation of ALP, but originated from a decrease in membrane permeability of the substrate molecules due to deswelling and collapse of the polymer layer above the LCST. As a consequence, inducing the synthesis of PNIPAM by triggering GOx activity in the silica colloidosomes gave rise to temperature-responsive membrane permeability and gated enzyme activity within the FeM-clay micro-compartments.

3. Conclusions

In conclusion, partially hydrophobic FeM-clay microparticles were prepared by surface methylation, and used as surface-active building blocks for the interfacial assembly of catalytic clay-based colloidosomes. The enclosed inorganic membrane was semi-permeable to small molecules such that enzyme reactions within the interior of the micro-compartments could be controlled by external regulation. As a consequence the FeM-clay colloidosomes have potential as a model of a synthetic protocell with dual catalytic functionality arising directly from the membrane building blocks themselves, and indirectly from the ability to encapsulate native enzymes.

When integrated into the colloidosome microstructure, the FeM-clay acts as an inorganic counterpart to horseradish peroxidase, functioning as a peroxidation catalyst in the presence of H_2O_2 to generate free radicals specifically at the membrane surface. We have demonstrated that this catalytic activity can not only be exploited to augment the properties of the colloidosome membrane by self-directed organic polymerization, but also

coupled to a H_2O_2 signal emanating from a coexistent population of GOx-containing silica colloidosomes. As a consequence, triggering the enzyme reaction in the population of silica colloidosomes remodels the membrane and generates new self-regulated membrane gating properties in the Fe-clay colloidosome population.

Although rudimentary in design, our studies indicate that new properties can be activated in subsets of colloidosome populations by chemical signaling within the synthetic community. Whilst we demonstrate a contemporary process involving the catalytic polymerization of NIPAM, there may be other emergent properties associated with artificial protocell communities that have closer relevance to fields such as the origin of life or prebiotic chemistry. In particular, we note that clay minerals exhibit selective absorption and enrichment of nucleotides,[29,30] provide photoprotection,[31] catalyze the synthesis of monomers and polymers of amino acids[32] and RNA,[33,34] and enhance genetic transcription.[35] The investigation of such properties within the context of protocell organization and collective behavior remains to be explored.

4. Experimental Section

Preparation of partially hydrophobic FeM-clay microparticles: Fe(III)-rich montmorillonite (FeM) (nontronite (NAu-2); Clay Source Repository, Clay Minerals Society; cation exchange capacity, 140 mmol 100 g^{-1}; total iron content, 23.4 wt%) was manually ground and suspended in aqueous 0.1 M NaCl solution adjusted to pH 2 using HCl, and left overnight. Fractions of the FeM-clay were collected by centrifugation at 3000 rpm, and chloride removed by repeated washing with doubly distilled water until the anion was not detected using $AgNO_3$. The clay suspension (10 g, 10% suspension in water) was mixed with hexadecyltrimethylammonium bromide (CTABr, 8.7 g), and the aqueous dispersion made up to a final volume of 250 mL and incubated at 80°C for 6h. The precipitate was collected by centrifugation and washed with 75% ethanol to remove free CTABr. The CTA-intercalated FeM clay was re-suspended in 100% acetonitrile and incubated at 80°C for 6h, and then centrifuged, washed with 75% ethanol, and redispersed in cyclohexane/water (75%) and maintained at 80°C until the dispersion became homogeneous. Methyl triethoxysilane (MTES, 2 mL) was added to the solution under stirring and the reaction mixture maintained at 80°C for 12 h. The modified FeM-clay was centrifuged, washed three times with 75% ethanol at pH 2 (adjusted by HCl to remove CTAB), and then three times with 100% ethanol. The resulting methylated FeM clay was resuspended in 100% cyclohexane prior to further use.

Preparation of FeM-clay colloidosomes: FeM-clay water-in-oil colloidosomes were prepared by a Pickering emulsion method typically using a water/oil volume fraction of 0.05, and

water/clay volume/weight ratio of 100 µL mg^{-1}. In general, 1 mg of the prepared partially hydrophobic FeM-clay was added to 2 mL of cyclohexane or dodecane. The dispersion was sonicated in an ultrasonic bath for 5 min, and then 100 µL of water or an aqueous solution containing various reagents (see below) was added followed by homogenization for one minute using a homogenizer (IKA, T18) at 10, 000 rpm. The resulting water-in-oil FeM-clay colloidosomes were transferred into a continuous water phase by cross-linking the inorganic membrane by reaction with TMOS, followed by treatment with a series of ethanol/water solvents. For this, 50 µL of TMOS was added to the oil phase of 2 mL of the Pickering emulsion, and the suspension gently mixed and left to stand on the bench at room temperature overnight. The top clear oil phase was replaced by 1 mL ethanol, and the dispersion subsequently centrifuged at 3000 rpm for 1 min and the top clear solution discarded. This procedure was repeated with graded ethanol/water mixtures, and the ethanol then replaced by a 10 mM Na-phosphate buffer (pH 6.7) for use of the colloidosomes in further experiments.

Encapsulation of aqueous solutes such as dye molecules, proteins or DNA within FeM-clay colloidosomes was undertaken by mixing 100 µL of an aqueous solution of fluorescein isothiocyanate (FITC; M_w = 389 g mol^{-1}; 0.01 mg mL^{-1}), rhodamine B (M_w = 479 g mol^{-1}; 0.01 mg mL^{-1}), calcein (M_w = 623 g mol^{-1}; 0.01 mg mL^{-1}), green fluorescent protein (GFP, M_w = 327,000 g mol^{-1}; 0.05 mg mL^{-1}), BSA (M_w = 665,000 g mol^{-1}; 0.05 mg mL^{-1}), alkaline phosphatase (ALP; M_w =140,000 g mol^{-1}; 100 µL, 10 U mL^{-1}; ≥1500 units mg^{-1}) or fluorescently tagged doubled-stranded DNA (SYBR green I; ≈2000 base pairs, M_w ≈ 13 x 10^6 g mol^{-1}) with 2 mL of dodecane containing 1 mg of the partially hydrophobic FeM-clay, followed by the procedures described above, except for enzyme assays involving ALP-containing colloidosomes, where an alkaline buffer (pH 9.5, 20 mM Tris, 20 mM Na-phosphate, 2 mM $ZnCl_2$ and 2 mM $MgCl_2$) was used.

FeM-clay-mediated polymerization of N-isopropylacrylamide: An aqueous suspension of FeM-clay microparticles (100 µL, 5 mg ml^{-1}) or preformed FeM-clay colloidosomes (200 µL, 25 mg ml^{-1}) was mixed with 2 mL of an aqueous solution of N-isopropylacrylamide (NIPAM) and PEG-diacrylate (PEG-DA) cross-linker at variable concentrations, and left unstirred at room temperature or 37°C for 0.5-24 h. Typically, poly(N-isopropylacrylamide) (PNIPAM) was prepared at a molar ratio of monomer NIPAM : PEG-DA of 20 : 1. In most experiments, fluorescein *o*-acrylate (FOA) was added to the reaction mixture, and co-polymerized with NIPAM and PEG-DA to produce materials suitable for examination with confocal and optical fluorescence microscopy.

Studies on membrane binding and permeability: 10 µL of an aqueous solution of FITC (0.01 mg mL^{-1}), rhodamine B (0.01 mg mL^{-1}), calcein (0.01 mg mL^{-1}), GFP (0.05 mg mL^{-1}), FITC-BSA

(0.05 mg mL^{-1}), or SYBR green I tagged (or stained) DNA was added to an aqueous suspension of buffer-containing FeM-clay colloidosomes (100 µL), and uptake or exclusion of the solutes monitored by fluorescence microscopy.

Preparation of protein-containing silica nanoparticle-stabilized colloidosomes: Partially hydrophobic silica nanoparticles with spherical morphology and primary mean diameter of 20–30 nm were prepared as described previously.[10,15] In brief, slica nanoparticle-stabilized colloidosomes were prepared as Pickering emulsions, cross-linked with tetramethoxysilane and transferred into water using methods described elsewhere.[15,18] Protein-containing silica colloidosomes were typically prepared by adding an aqueous solution (total volume, 500 µL) containing Na-phosphate buffer (10 mM, pH 7.2), glucose oxidase (GOx; M_w =160,000 g mol^{-1}, 200 µL, 200 U mL^{-1}) and Rhodamine B-labeled bovine serum albumin (RhB-BSA; 10 µL, 5 mg mL^{-1}) to 10 mL of cyclohexane containing 100 mg of partially hydrophobic silica nanoparticles.

Signal-induced polymer synthesis and gated enzyme reactions in mixed colloidosome populations: Aqueous suspensions of alkaline phosphatase (ALP)-containing FeM-clay colloidosomes (200 µL, 25 mg mL^{-1}) and GOx-containing silica nanoparticle-stabilized colloidosomes (40 µL, 10 mg mL^{-1}) were mixed at room temperature, and an aqueous solution of NIPAM (2.5 %), PEG-DA (0.125%) and FOA (1 µL, 1 mM) added. Glucose (40 µL, 0.1M) was then added to the mixture to initiate the cascade reaction. Typically, the reaction was left for 24 h to produce mixtures of PNIPAM-coated FeM-clay colloidosomes and silica colloidosomes.

The influence of signal-induced polymer synthesis and assembly formation on the activity of ALP molecules encapsulated within the PNIPAM/FeM-clay colloidosomes was investigated by monitoring the temperature-dependent ALP-mediated dephosphorylation of 4-nitrophenyl phosphate (pNPP) in alkaline buffer. An aqueous solution of pNPP (10 µL, 10 mM) was added to the mixed colloidosome population after 24 h of reaction time, and the initial rates of ALP-mediated dephosphorylation associated with production of the yellow product 4-nitrophenolate (absorption band 405 nm, extinction coefficient = 18.1 mM^{-1} cm^{-1}) from the PNIPAM/FeM-clay colloidosomes determined at temperatures between 25 and 40°C by UV-vis spectroscopy. Similar experiments were undertaken using mixed suspensions of GOx-containing silica colloidosomes and ALP-containing polymer-free FeM-clay colloidosomes dispersed in a buffered solution of all the cascade reactants except for NIPAM.

Characterization: X-ray diffraction (XRD) profiles of FeM-clay samples were collected on a D8 Advance Bruker diffractometer with a small angle accessory from 1.6 to 15 degrees

using CuKa radiation (λ=1.5406Å). The particle size distributions were determined from optical microscope and Scanning Electron Microscope (SEM) images. Morphological characterizations were performed on a IT300 SEM using a 20 kV or Ultra 55 FESEM and a 15 kV accelerating voltage. FTIR ATR spectra were collected on a Perkin-Elmer model Spectrum One spectrometer equipped with a micro-ATR unit. Optical microscopy observations were performed on a Leica DMI3000 B manual inverted fluorescence microscope or DMI6000 automotive inverted epifluorescence microscope. Two band pass filters were used: excitation at 450–490 nm with an emission cut off at 510 nm (I3), and excitation at 515–560 nm with an emission cut off at 580 nm (N2.1). Confocal laser scanning microscopy observations were performed on a Leica SP 7 inverted confocal laser scanning microscope. UV-vis spectra were collected on a Perkin-Elmer Lambda 25 spectrophotometer. The aqueous Fe clay particle size distribution were measured using a Zetasizer Nano ZS90. Contact angles of water droplets mounted on FeM-clay particles before or after treatment with methyltriethoxysilane were determined using a Kruss DSA30 system.

Acknowledgments

We thank the ERC Advanced Grant scheme (S.M.) for financial support. The work was partly supported by the National Natural Science Foundation of China (Nos. 41472310 and 41130746), the Chinese Ministry of Science and Technology (No. 2014CB846003). S. Sun is grateful for financial support from the China Scholarship Council.

References

[1] K. Renggli, P. Baumann, K. Langowska, O. Onaca, N. Bruns, W. Meier, *Adv. Funct. Mater.* **2011**, *21*, 1241.

[2] B. Städler, A. D. Price, R. Chandrawati, L. Hosta-Rigau, A. N. Zelikin, F. Caruso, *Nanoscale.* **2009**, *1,* 68.

[3] V. Noireaux, Y. T. Maeda, A. Libchaber, *Proc. Natl. Acad. Sci. U. S. A.* **2011**, *108*, 3473.

[4] M. Li, X. Huang, T. Y. D. Tang, S. Mann, *Curr. Opin. Chem. Biol.* **2014**, *22*, 1.

[5] D. Lee, D. A. Weitz, *Adv. Mater.* **2008**, *20*, 3498.

[6] K. Zhang, W. Wu, K. Guo, J. Chen, P. Zhang, *Langmuir* **2010,** *26*, 7971.

[7] M. Okada, H. Maeda, S. Fujii, Y. Nakamura, T. Furuzono, *Langmuir* **2012**, *28*, 9405.

[8] J. S. Sander, A. R. Studart, *Langmuir* **2013**, *29*, 15168.

[9] T. Bollhorst, T. Grieb, A. Rosenauer, G. Fuller, M. Maas, K. Rezwan, *Chem. Mater.* **2013**, *25*, 3464.

[10] B. P. Binks, R. Murakami, *Nat. Mater.* **2006**, *5*, 865.

[11] C. Huo, M. Li, X. Huang, H. Yang, S. Mann, *Langmuir* **2014**, *30*, 15047.

[12] Y. Yang, Z. Liu, D. Y. Wu, M. Wu, Y. Tian, Z. W. Niu, Y. Huang, *J. Colloid Interf. Sci.* **2013**, *410*, 27.

[13] M. Williams, S. P. Armes, *Langmuir* **2012**, *28*, 1142.

[14] C. Wu, S. Bai, M. B. Ansorge-Schumacher, D. Wang, *Adv. Mater.* **2011**, *23*, 5694.

[15] M. Li, D. C. Green, J. L. R. Anderson, B. P. Binks, S. Mann, *Chem. Sci.* **2011**, *2*, 1739.

[16] R. K. Kumar, M. Li, S. N. Olof, A. J. Patil, S. Mann, *Small* **2013**, *9,* 357.

[17] M. Li, X. Huang, S. Mann, *Small* **2014***, 10,* 3291.

[18] M. Li, R. L. Harbron, J. V. M. Weaver, B. P. Binks, S. Mann, *Nat. Chem.* **2013**, *5,* 529.

[19] A. B. Subramaniam, J. Wan, A. Gopinath, H. A. Stone, *Soft Matter* **2011**, *7*, 2600.

[20] R. F. A. Teixeira, H. S. McKenzie, A. A. Boyd, S. A. F. Bon, *Macromolecules* **2011**, *44*, 7415.

[21] N. P. Ashby, B. P. Binks, V. N. Paunov, *Phys. Chem. Chem. Phys.* **2004**, *6*, 4223.

[22] P. H. R. Keen, N. K. H. Slater, A. F. Routh, *Langmuir* **2014**, *30*, 1939.

[23] O. J. Cayre, S. Biggs, *J. Mater. Chem.* **2009**, *19*, 2724.

[24] M. Pang, A. J. Cairns, Y. Liu, Y. Belmabkhout, H. C. Zeng, M. Eddaoudi, *J. Am. Chem. Soc.* **2013**, *135*, 10234.

[25] J. Faria, M. Ruiz, D. E. Resasco, *Adv. Synth. Catal.* **2010**, *352*, 2359.

[26] S. Crossley, J. Faria, M. Shen, D. E. Resasco, *Science* **2010**, *327*, 68.

[27] D. Liu, H. Dong, M. E. Bishop, H. Wang, A. Agrawal, S. Tritschler, D. D. Eberl, S. Xie, *Geochim. Cosmochim. Acta.* **2011**, *75*, 1057.

[28] D. Liu, H. Dong, M. E. Bishop, I. Zhang, H. Wang, S. Xie, S. Wang, L. Huang, D. D. Eberl, *Geobiology* **2012**, *10*, 150.

[29] C. Feuillie, I. Daniel, L. J. Michot, U. Pedreira-Segade, *Geochim. Cosmochim. Acta* **2013**, *120*, 97.

[30] O. Poch, M. Jaber, F. Stalport, S. Nowak, T. Georgelin, J. F. Lambert, C. Szopa, P. Coll, *Astrobiology* **2015**, *15*, 221.

[31] E. Biondi, S. Branciamore, M. C. Maurel, E. Gallori, *Bmc Evol. Biol.* **2007**, ***7***, S2.

[32] M. Jaber, T. Georgelin, H. Bazzi, F. Costa-Torro, J. F. Lambert, G. Bolbach, G. Clodic, *J. Phys. Chem. C* **2014**, *118*, 25447.

[33] W. Huang, J. P. Ferris, *J. Am. Chem. Soc.* **2006**, *128*, 8914.
[34] M. F. Aldersley, P. C. Joshi, J. D. Price, J. P. Ferris, *Appl. Clay Sci.* **2011**, *54*, 1.
[35] D. Yang, S. Peng, M. R. Hartman, T. Gupton-Campolongo, E. J. Rice, A. K. Chang, Z. Gu, G. Q. Lu, D. Luo, *Sci. Rep.* **2013**, *3*, 3165.

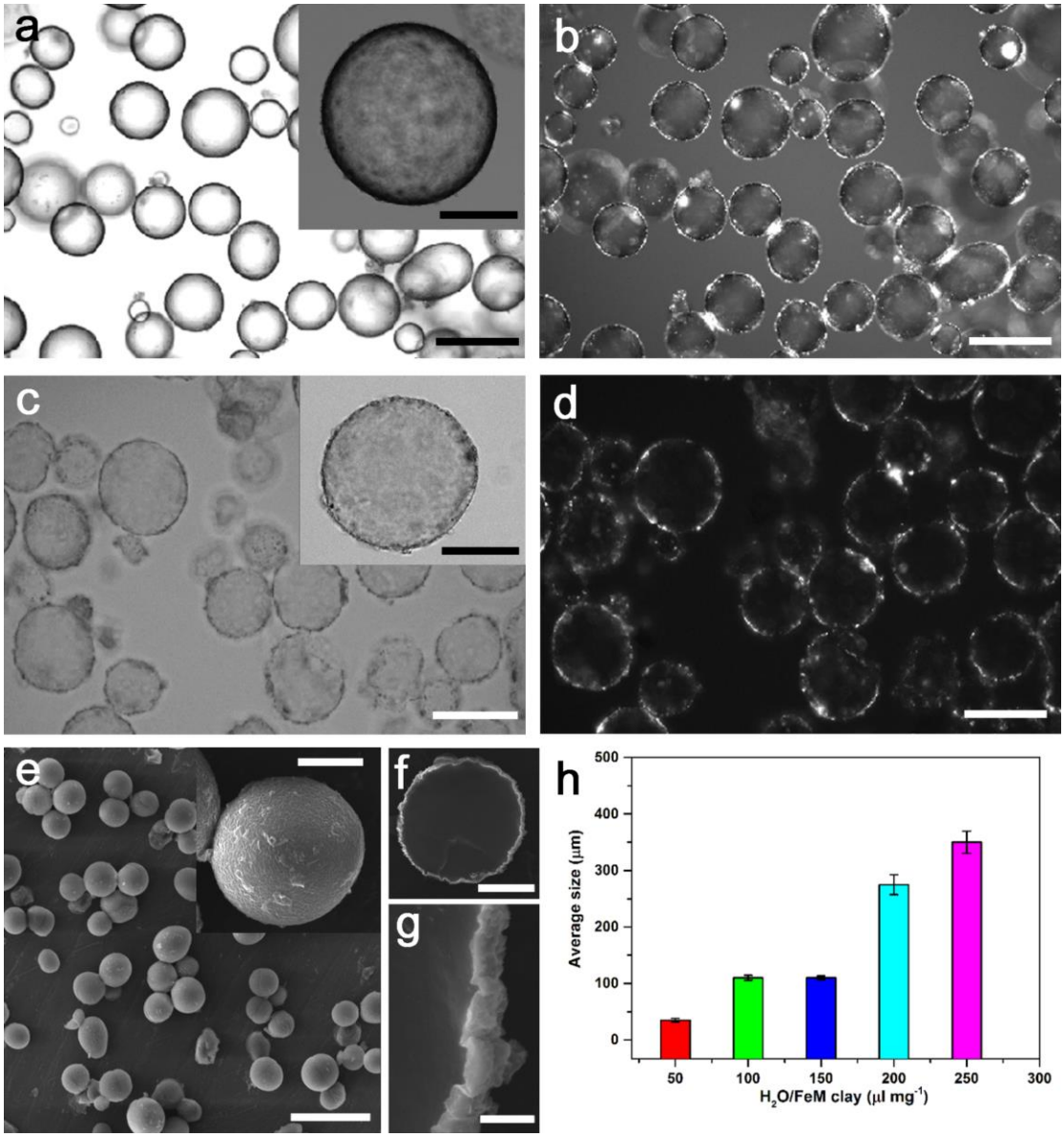

Figure 1. (**a-d**) Optical microscopy (**a,c**) and corresponding polarized light microcopy (**b,d**) images showing birefringent FeM-clay colloidosomes before (**a,b**) and after (**c,d**) transfer from oil into water. Samples were prepared at a water/oil volume fraction of 0.05, and water/clay volume/weight ratio of 100 µL mg^{-1}. Insets in (**a**) and (**c**) show individual colloidosomes suspended in oil or water, respectively; scale bars: (**a,b**) 200 µm, 150 µm (inset); (**c,d**) and inset, 100 µm. (**e**) SEM image of dried intact FeM-clay colloidosomes; inset shows individual colloidosome; scale bars, 100 µm and 20 µm (inset). (**f,g**) SEM images of a single freeze-fractured FeM-clay colloidosome showing hollow interior (**f**) and continuous clay membrane (**g**); scale bars: 40 µm (**f**), and 5 µm (**g**). (**h**) Plot showing change in mean diameter of FeM-clay colloidosomes prepared at different water/clay volume/weight ratios.

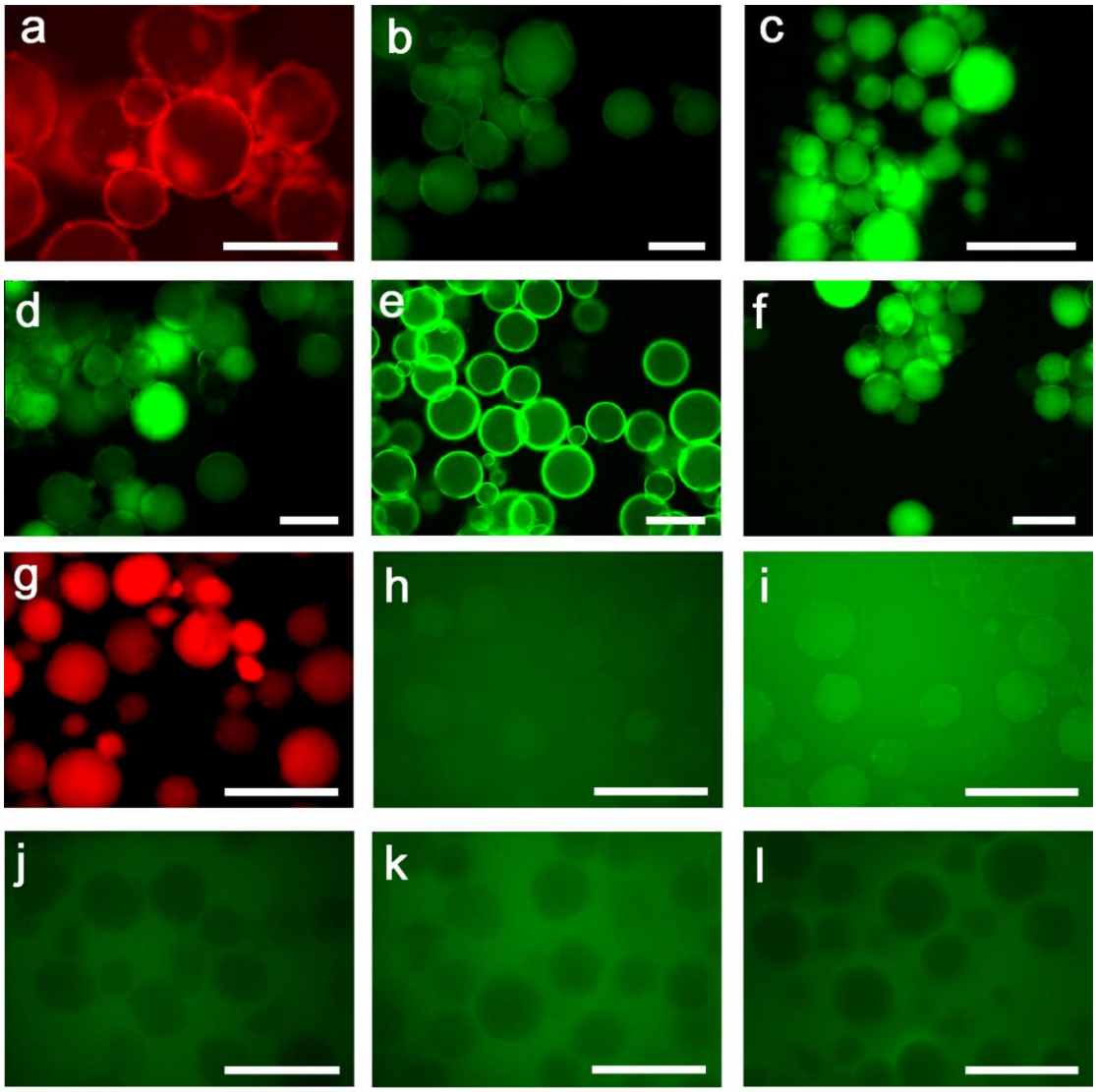

Figure 2. (**a-f**) Fluorescence microscopy images showing encapsulation of Rhodamine B (**a**), FTTC (**b**), calcein (**c**), GFP (**d**), FITC-BSA (**e**) and SYBR green I-stained DNA (**f**) in FeM-clay water-in-oil colloidosomes. (**g-l**) Fluorescence microscopy images of water-in-water FeM-clay colloidosomes showing membrane binding of Rhodamine B (**g**), passive uptake of FTTC (**h**) and calcein (**i**) into the micro-capsule interior, and exclusion of membrane-impermeable GFP (**j**), FITC-BSA (**k**) and SYBR green I-stained DNA (**l**). The contrast in images (**h,i**) is low because the sequestered fluorescent solutes are also present in the continuous water phase. Virtually no green fluorescence is observed inside the colloidosomes in (**j-l**) indicating that solutes in the continuous water phase (green fluorescence) do not diffuse into the micro-capsules. Samples were prepared at a water/oil volume fraction of 0.05, and water/clay volume/weight ratio of 100 µL mg^{-1}. All scale bars, 200 µm.

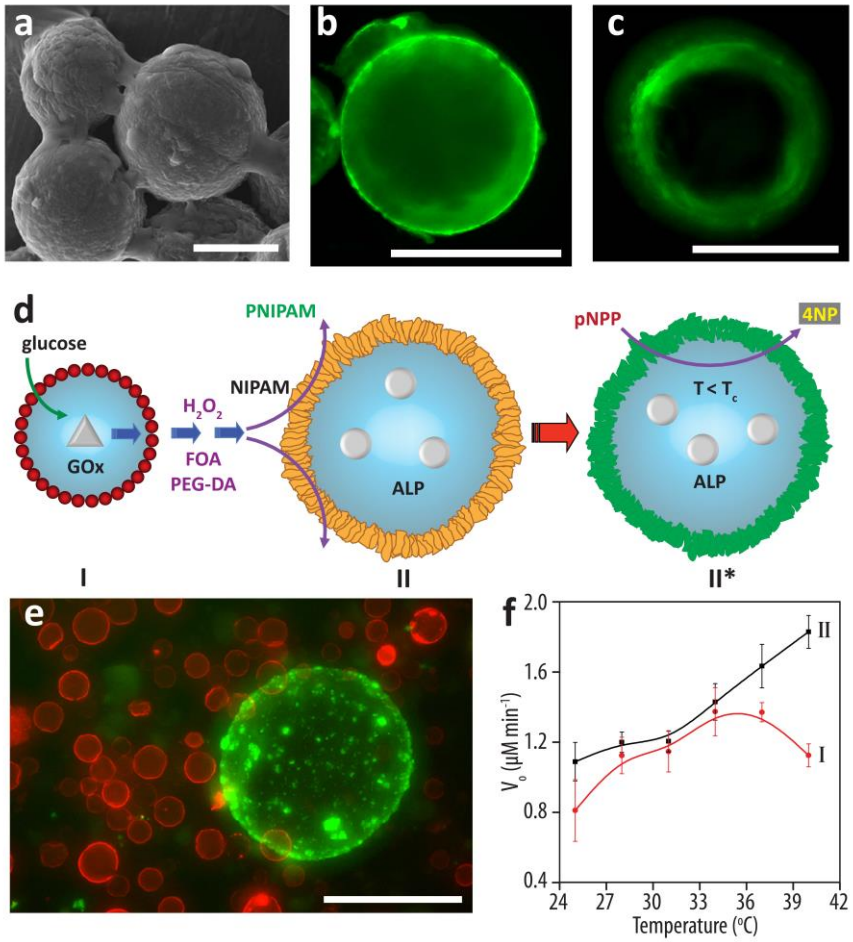

Figure 3. (**a**) SEM image of dried FeM-clay colloidosomes after polymerization for 24 h showing adherent PNIPAM surface film; scale bar, 40 µm. (**b,c**) Fluorescence microscopy micrographs of PNIPAM/FeM-clay colloidosomes prepared by self-directed oxidative catalysis and imaged at room temperature (**b**) or at 37°C (**c**) showing increased fluorescence intensity associated with deswelling of the membrane-linked polymer above the LCST. The reaction time was 24 h; scale bars, 150 µm and 200 µm, respectively. (**d**) Scheme showing chemical communication and functional adaptation in colloidosome communities. Addition of glucose to silica colloidosomes (population **I,** red) containing GOx (triangle) generates a H_2O_2 signal that diffuses to larger FeM-clay colloidosomes (population **II**, orange), which then catalytically polymerize NIPAM in the presence of FOA and PEG-DA to produce a green fluorescent PNIPAM shell specifically on the inorganic membrane (population **II***, green). Population **II** contains ALP (circles) and dephosphorylation of membrane permeable pNPP to 4NP becomes gated in **II*** after signal-induced polymerization if the temperature (T) is below the LCST (T_c). (**e**) Fluorescence microscopy image of a mixed population of red fluorescent RhB-BSA/GOx-containing silica colloidosomes and ALP-containing FeM-clay colloidosomes in the presence of NIPAM, FOA (1%) and PEG-DA, and recorded 24 h after addition of glucose showing emergence of green PNIPAM/FeM-clay colloidosomes in the binary community via GOx-induced release of H_2O_2 and signaling of clay-catalysed polymerization; scale bar, 150 µm. (**f**) Temperature dependent plots of initial velocity (V_0) of ALP-mediated pNPP dephosphorylation for PNIPAM/FeM-clay colloidosomes (**I**, red plot) and as-prepared FeM-clay colloidosomes (**II**, black plot).